physica status solidi a
www.pss-a.com

Fe-Related Defects in Si: Laplace Deep-Level Transient Spectroscopy Studies

*Katarzyna Gwozdz and Vladimir Kolkovsky**

Herein, the electrical properties of Fe-related defects in hydrogenated n- and p-type Si doped with iron during the crystal growth in a vacancy mode are investigated. Six deep-level transient spectroscopy (DLTS) peaks labeled Fe_i, FeB, CH, $E125_{FeH}$, $E145_{Fe}$, and $E240_{Fe}$ are observed in as-grown n- and p-type Si after wet chemical etching (WCE). By comparing the electrical properties of the defects with those previously reported in the literature, Fe_i is correlated with interstitial iron, FeB with an iron–boron complex, and C–H with a carbon–hydrogen complex in Si. No traces of the peak previously assigned to the single donor state of Fe_iH are observed after reverse bias annealing at 110 °C in hydrogenated Si. By analyzing the depth profiles of the defects in n-type Si, it is shown that $E125_{FeH}$ comprises only one H atom. The electrical and annealing properties of $E125_{FeH}$, $E145_{Fe}$, and $E240_{Fe}$ are investigated and their origin is discussed.

1. Introduction

Iron-related defects could be introduced into silicon in various processing steps as unintentional contamination. They can act as effective minority carrier generation centres, which influence the leakage current in reverse-biased junctions or reduce the minority carrier diffusion length, leading to the degradation of the solar cells' efficiency.[1] According to theory, substitutional (Fe_S) and interstitial iron (Fe_i) should introduce electrical levels into the bandgap of Si. However, only the single donor state of Fe_i with an activation energy of about 0.40 ± 0.05 eV above the valence band was experimentally observed in p-type Si, whereas until now no deep levels were correlated with Fe_S in the band gap of Si. Interstitial iron is already mobile at room temperature and it can interact with different impurities.[1] More than 30 Fe-related complexes were detected by electron paramagnetic resonance (EPR) in Si and almost 25 energy levels of Fe-related defects were reported in the bandgap of Si in different studies.[1]

The interaction of interstitial and substitutional Fe with H is not well understood. Theory predicts the existence of two electrical levels of Fe_iH and one level of Fe_SH in the bandgap of Si, although their positions vary in different studies.[2–4] Experimentally, no levels of Fe_iH-related defects were reported in p-type Si hydrogenated by dc H-plasma, H-implantation, or wet chemical etching (WCE) in other studies.[5–9] In contrast, Sadoh et al.[10] correlated a defect level with an activation energy of 0.31 eV above the valence band with the single donor state of Fe_iH in hydrogenated n-type Si using thermally stimulated capacitance experiments (TSCAP) combined with minority carrier injection. The existence of this defect level was also confirmed by deep-level transient spectroscopy (DLTS) measurements in p-type Si hydrogenated from a SiN layer which was grown by direct plasma-enhanced chemical vapor deposition, but the defect level appeared only after reverse bias annealing (RBA) at around 110 °C.[11] This was explained by assuming that during RBA, positively charged H atoms drift toward the bulk of p-type Si, where they can interact with shallow acceptors or other crystal imperfections.

In the present study, we investigate the electrical properties of Fe-related defects in hydrogenated n- and p-type Si using DLTS and minority carrier transient spectroscopy (MCTS) measurements. In contrast to the previous studies, we introduced iron into Si during the growth by the float-zone (FZ) method in a vacancy mode. Several DLTS peaks were detected in these samples and their electrical properties will be analyzed. The depth profiles of these defects indicate that a dominant peak is correlated with a FeH-related defect with one H atom whereas two other deep traps belong to different charge states of another defect. The origin of the defects will be discussed.

2. Results

Figure 1 shows a DLTS spectrum recorded in the Fe-doped n-type Si sample after WCE (black line). Four DLTS peaks labeled CH, $E125_{FeH}$, $E145_{Fe}$, and $E240_{Fe}$ were observed in this sample. The intensities of CH and $E125_{FeH}$ were significantly larger when measured close to the surface in comparison with those

K. Gwozdz
Department of Quantum Technologies
Faculty of Fundamental Problems of Technology
Wroclaw University of Science and Technology
Wybrzeze Wyspianskiego 27, 50-370 Wroclaw, Poland

V. Kolkovsky
Fraunhofer IPMS
EMT
Maria-Reiche Str. 2, 01109 Dresden, Germany
E-mail: uladzimir.kalkouski@ipms.fraunhofer.de

The ORCID identification number(s) for the author(s) of this article can be found under https://doi.org/10.1002/pssa.202200139.

DOI: 10.1002/pssa.202200139

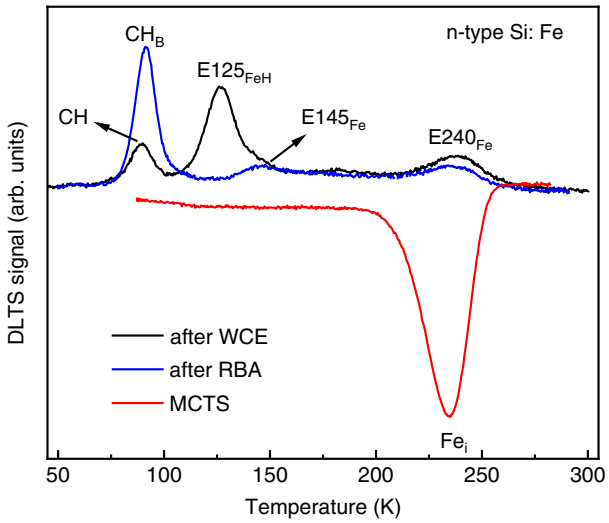

Figure 1. DLTS (black line) and MCTS (red line) spectra recorded in n-type Si doped with Fe after WCE. A typical DLTS spectrum recorded in the same sample after RBA with a reverse bias of −5 V for 30 min at 110 °C is also shown (blue line).

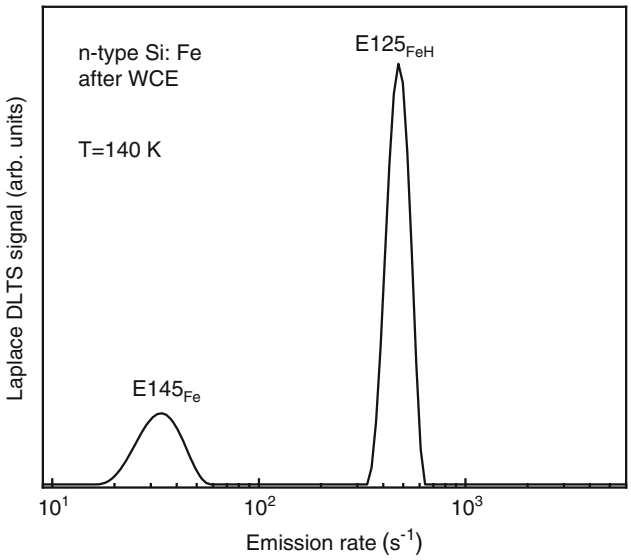

Figure 2. Laplace DLTS spectra recorded in hydrogenated n-type Si doped with Fe at 140 K.

observed in the bulk of Si. Both CH and E125$_{FeH}$ anneal out with or without reverse bias applied to the diode (blue line in Figure 1) already at around 110 °C. In contrast, both E145$_{Fe}$ and E240$_{Fe}$ were also observed in the annealed sample. Besides these peaks, another defect labeled CH$_B$ appears in the DLTS spectrum after RBA. The electrical properties of CH and CH$_B$ are similar to those reported by Stübner et al.[12] and therefore we correlate them with the single-acceptor state of the carbon–hydrogen pair and the single donor state of a complex containing C and several H atoms, respectively. Both E145$_{Fe}$ and E240$_{Fe}$ anneal out simultaneously at about 200 °C. The presence of deep levels in the lower part of the bandgap was probed with MCTS measurements in hydrogenated n-type Si. Due to technical limitations, we were able to perform these measurements only after a couple of days of keeping the sample at room temperature. Only one MCTS peak with a maximum at about 230 K dominates the spectrum (see the red line in Figure 1).

Figure 2 shows a Laplace DLTS spectrum recorded at 140 K in hydrogenated n-type Si. Two Laplace DLTS peaks labeled E125$_{FeH}$ and E145$_{Fe}$ were observed in this spectrum. The intensity of E125$_{FeH}$ was significantly larger than that of E145$_{Fe}$ when measuring close to the surface of the sample, whereas their intensities became comparable deeper in the bulk of Si.

Table 1. Electrical properties of CH and Fe-related defects observed in this study. The activation enthalpy and the apparent capture cross section σ_a were determined by Laplace DLTS from the Arrhenius plot (ln (emission rate/T^2 vs $1/T$)).

Labeling of energy levels	Activation enthalpy	Apparent capture cross section [cm^2]	Level identification
CH	E_C−0.15 eV	1.4×10^{-16}	CH (−/0)
E125$_{FeH}$	E_C−0.22 eV	3.2×10^{-16}	Fe$_i$H (−/0)
E145$_{Fe}$	E_C−0.25 eV	3.2×10^{-16}	Fe$_S$-unknown impurity (−/0)
E240$_{Fe}$	E_C−0.53 eV	2.7×10^{-14}	Fe$_S$-unknown impurity (0/+)

Figure 3a shows a typical DLTS spectrum recorded in hydrogenated p-type Si before and after RBA with a reverse bias of −4 V at 110 °C. After WCE, a single DLTS peak labeled FeB was observed at about 55 K. The intensity of this peak decreases significantly after RBA performed at 110 °C while another peak labeled Fe$_i$ appears in the DLTS spectrum at about 240 K. The concentration of Fe$_i$ was obtained from Laplace DLTS measurements and it was around 2×10^{12} cm^{-3}. The electrical properties of the defects corresponding to these peaks are consistent with those of interstitial iron (Fe$_i$) and the iron–boron pair (FeB), as previously reported in the literature.[1] The reduction of the intensity of FeB after RBA in Figure 3 could be explained with the breakup of these pairs at elevated temperatures and the following separation of interstitial Fe from substitutional boron in applied electric field during annealing. One should also note that similar DLTS spectra were observed after WCE and after dc H plasma treatment in p-type Si. To estimate the H concentration introduced after WCE, we also recorded the depth profiles of the free carrier concentration in hydrogenated p-type Si before and after RBA (Figure 3b). The doping level in the bulk of Si was around 8×10^{13} cm^{-3} and it decreases toward the surface in the hydrogenated Si sample. We correlate this decrease with the passivation of shallow acceptors by positively charged H.[13] The annealing of p-type Si with a reverse bias at elevated temperatures leads to the breakup of BH complexes and several other H-related defects. Due to the applied electric field, the free H drifts toward the bulk of Si. At the end of the space–charge region of the diode, where the electric field is weak, H starts to interact with substitutional boron by passivating it. The passivation of electrically active B leads to a significant dip in the free carrier concentration profile at around 10 μm below the surface. The H concentration in this depth could be derived from the magnitude of this dip as around 2×10^{13} cm^{-3}. In our previous studies we showed that such concentrations of H introduced after WCE were high enough to observe various CoH_x, NiH_x, and TiH_x complexes with $x \leq 3$.[14–17]

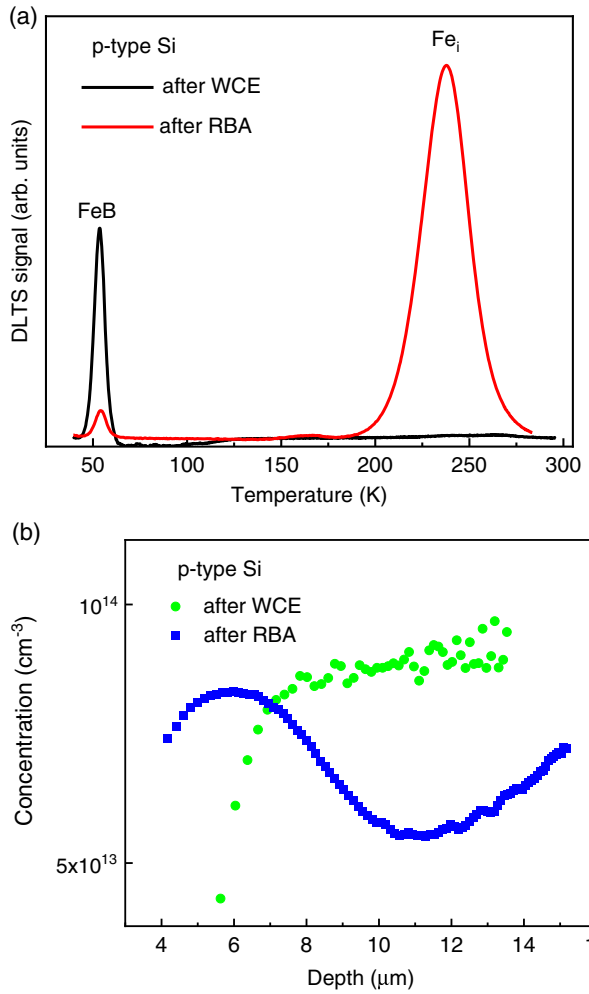

Figure 3. DLTS spectra recorded in p-type Si doped with Fe after WCE and after the following RBA performed with a reverse bias of −5 V for 30 min at 110 °C. The inset shows the depth profiles of free carrier concentration in the same sample before and after RBA.

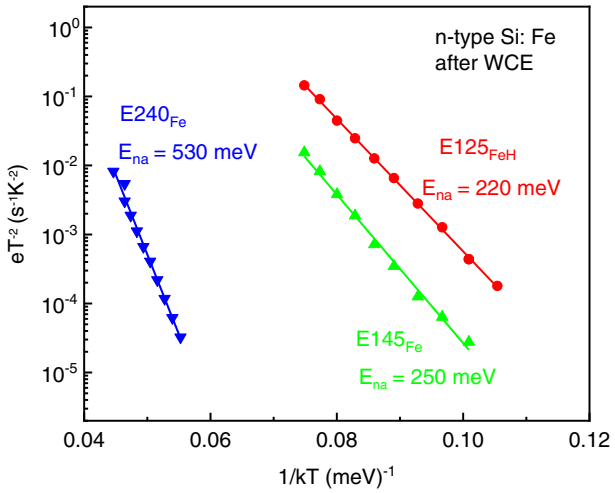

Figure 4. Arrhenius plots of the traps observed in Figure 1 and 2. The activation enthalpy is given in meV below the conduction band.

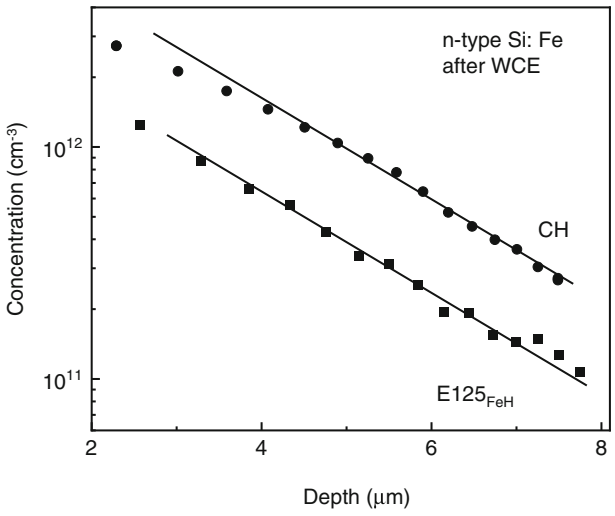

Figure 5. Concentration depth profiles of CH and E125$_{FeH}$. The solid lines are fits to the defect concentrations at larger depth.

Figure 4 presents Arrhenius plots obtained from the shift of the emission rate of the majority traps observed in n-type Si as a function of temperature (see also **Table 1**). We do not show the Arrhenius plots recorded for CH, CH$_B$, FeB, and Fe$_i$ as they are similar to those reported previously in the literature.[1,12]

Depth profiles of CH and E125$_{FeH}$ recorded in n-type Si after WCE are shown in **Figure 5**. The concentration of both defects is descending toward the bulk of Si. The solid lines are a guide for the eye and they demonstrate that the decrease in the concentration of CH and E125$_{FeH}$ is identical. The intensities of E145$_{Fe}$ and E240$_{Fe}$ were relatively small in n-type Si and thus it was not possible to obtain reliable depth profiles of these defects.

3. Discussion

Besides the well-known CH,[12] CH$_B$,[12] FeB,[1] and Fe$_i$,[1] three additional deep electron traps labeled E125$_{FeH}$, E145$_{Fe}$, and E240$_{Fe}$ were observed in the upper half of the bandgap of hydrogenated n-type Si doped with Fe. Several Fe-related defects were also previously reported after the iron diffusion at around 1000–1200 °C in n-type Si in the literature and they were attributed to interstitial Fe clusters,[18] Fe$_i$ complexes,[19] or Fe-related defects.[20] However, the electrical properties of the defects differ significantly from those of E125$_{FeH}$, E145$_{Fe}$, and E240$_{Fe}$ observed in the present study and therefore they belong to different defects. We did not observe E125$_{FeH}$, E145$_{Fe}$, and E240$_{Fe}$ in samples without Fe and, therefore, we attribute these levels to Fe-related defects.

The determination of the depth profiles of E145$_{Fe}$ and E240$_{Fe}$ was hindered by their low intensity but their concentration obtained from the DLTS spectrum was identical after WCE and after annealing performed at 110 °C. Because of this and their simultaneous disappearance after RBA, we assign these peaks to different charge states of the same defect. In a

dislocation-free CZ Si or FZ Si, vacancies or self-interstitials could be incorporated during the crystal growth. According to Voronkov's criteria,[21] vacancies should be generated in Si pulled with a ratio of velocity over axial temperature gradient larger than a certain critical value, whereas self-interstitial atoms should be created if this condition is not fulfilled. The samples used in the present study were grown under conditions, which prefer the formation of vacancies in these samples. It is therefore reasonable to assume that the codoping of these samples with Fe during growth leads to the interaction of Fe with Si vacancies, forming substitutional Fe. The concentration of $E145_{Fe}$ and $E240_{Fe}$ is significantly lower than that of Fe_i or FeB and we did not observe any correlation between these defects. Therefore, we attribute $E145_{Fe}$ and $E240_{Fe}$ to substitutional Fe-related defects in our samples. Previously, the existence of Fe_S or (111)-distorted Fe_S was reported using Mössbauer spectroscopy,[22] emission channeling techniques,[23] and EPR[24] in electron- or ion-irradiated Si samples. However, no energy positions of these levels were reported in the literature and therefore we are not able to conclude whether $E145_{Fe}$ and $E240_{Fe}$ might be correlated with these defects. One should also note that theory predicts the existence of only a single acceptor state of isolated Fe_S at about 0.4 eV below the conduction band of Si,[25] and the annealing temperature of $E145_{Fe}$ and $E240_{Fe}$ at around 200 °C is relatively low for the annealing of isolated substitutional transition metal (TM) species in Si. This is contradictory to the assignment of $E145_{Fe}$ and $E240_{Fe}$ to different charge states of isolated substitutional Fe. Therefore, we tentatively correlate these defects with complexes, which contain Fe_S and an unknown impurity in Si. However, further studies are necessary to shed light on the origin of the defect.

The concentration of $E125_{FeH}$ is descending toward the bulk of Si and its intensity is highest close to the surface of Si. According to the findings of Feklisova and Yarykin,[26] the identical slopes of the reduction of the concentrations of CH and $E125_{FeH}$ demonstrate that similarly to CH $E125_{FeH}$ contains a single H atom. One should note that the intensity of $E125_{FeH}$ is significantly larger in comparison with those of $E145_{Fe}$ and $E240_{Fe}$ and they rather stem from different defects. In contrast, the concentration of Fe_i also lies at around $2 \times 10^{12}\,cm^{-3}$. In good agreement with theory,[2,4] we assign $E125_{FeH}$ to the single acceptor state of Fe_iH. The annealing temperature of this defect at around 300–350 K is also consistent with this assignment since many other TM–H complexes anneal out at similar temperatures.[14–17,27,28]

As mentioned in the introduction, another deep trap with an activation energy at about 0.31 eV above the valence band was attributed to the single donor state of Fe_iH in other studies[10,11] using TSCAP measurements combined with minority carrier injection and DLTS measurements in n- and p-type Si, respectively. However, the thermal stability of $E125_{FeH}$ and the traps observed in other studies[10,11] differ significantly. $E125_{FeH}$ anneals out already after a week at RT, whereas the traps assigned to the donor states of Fe_iH in other studies[10,11] are significantly more stable although they were also reported to anneal out at different temperatures: at around 175 °C in n-type Si[10] and at around 125 °C in p-type Si.[11] One should also note that we did not observe any traces of a level at about 0.31 eV above the valence band by MCTS and DLTS measurements after RBA in hydrogenated n-type and p-type Si, respectively. Similarly, no traces of this defect were previously observed after RBA in hydrogenated p-type Si doped with Fe in the study by Feklisova et al.[9] Leonard et al.[11] suggested that the absence of this defect in p-type Si in the study by Feklisova et al.[9] and its observation in the study by Leonard et al.[11] could be explained by different concentrations of H introduced in a different way in different studies. According to their explanation, a significantly smaller concentration of H should be introduced in Si samples hydrogenated by WCE in comparison with that after diffusion of H from silicon nitride layers deposited on the top of Si in the study by Leonard et al.[11] However, the level at $E_V + 0.31$ eV was also detected after RBA in n-type Si hydrogenated by WCE in the study by Sadoh et al.,[10] whereas we did not also observe any traces of H-related defects in p-type Si hydrogenated by a dc H plasma treatment, which introduces more H in comparison with that by WCE. Finally, the concentration of H introduced after WCE was high enough to detect many other TM–H-related complexes even without RBA in n- and p-type Si.[14–17,27,28]

One should also emphasize that the single donor states of CH and COH complexes in p-type Si[29,30] have also similar electrical properties to the defects observed at $E_V + 0.31$ eV in other studies.[10,11] Both CH and COH appear in samples with a high C concentration or in hydrogenated CZ samples with high C and O concentrations, respectively. Moreover, we were not able to detect these defects in Si samples hydrogenated by WCE[29] and the introduction of high H concentrations was necessary to observe them. The concentration of C and O is unknown in samples used for the investigation in other studies[10,11] but they were grown in a different way. It is well known that the O content in FZ samples used in the study by Sadoh et al.[10] is significantly lower in comparison with those grown by the CZ technique used for the investigations in the study by Leonard et al.[11] Then different annealing temperatures of the defects observed at $E_V + 0.31$ eV in other studies[10,11] could be explained by their different origins and they might be correlated with the CH[10] and COH[11] complexes. However, further studies are necessary to confirm or refute this hypothesis.

In the present study, several traps labeled CH, $E125_{FeH}$, $E145_{Fe}$, $E240_{Fe}$, FeB, and Fe_i were observed in hydrogenated n- and p-type Si doped with Fe during the growth. By comparing the electrical properties of CH, FeB, and Fe_i with those known from the literature, we assign these defects to a carbon–hydrogen complex, an iron–boron complex, and interstitial iron, respectively. The identical concentrations of $E145_{Fe}$ and $E240_{Fe}$ indicate that both defects belong to different charge states of the same Fe-related defect. We tentatively assign this deep trap to Fe_S-related defect. By comparing depth profiles of $E125_{FeH}$ and CH, we conclude that $E125_{FeH}$ contains a single H atom and we attribute this defect to the single acceptor state of Fe_iH.

4. Experimental Section

Both p- and n-type Si samples doped with boron and phosphorous, respectively, were cut from Fe-doped FZ wafers. The doping level was around $1.7 \times 10^{14}\,cm^{-3}$ in n-type Si and around $8 \times 10^{13}\,cm^{-3}$ in p-type Si. Hydrogen was introduced by WCE in CP4A ($HF:HNO_3:CH_3COOH$ 3:5:3) at room temperature or by remote dc plasma at 323 or 373 K

for 60 min. Schottky contacts were made by resistive evaporation of Au or Al through a shadow mask onto the polished side of the n- or p-type sample, respectively. Ohmic contacts were made by rubbing a eutectic InGa alloy onto the backside of the samples. The quality of the Schottky and Ohmic contacts was checked by current–voltage and capacitance–voltage (*C*–*V*) measurements at room temperature and at 50 K. The *C*–*V* curves were recorded at 1 MHz. Conventional DLTS, MCTS, and high-resolution Laplace DLTS were used to investigate the electrical properties of the defects. The peak labeling in this work corresponded to the DLTS peak maximum temperature at an emission rate of 47 s^{-1} and described the assignment of the defect. Several samples were annealed with or without reverse bias at different temperatures. The concentration depth profiles of the levels were measured by Laplace DLTS in the double-pulse mode, as described in the study by Dobaczewski et al.[31] For the determination of the defect concentration, the temperature-dependent λ-layer was taken into account.[32]

Acknowledgements

The authors thank Dr. Abrosimov for supplying the samples with iron introduced during the growth. K.G. would like to thank the statutory grant (no. 8211104160) of Department of Quantum Technologies of Wroclaw University of Science and Technology and DAAD for the support of her stay in Dresden. V.K. also thanks Dr. Stübner for the careful reading of the manuscript and his valuable comments and Professor Weber for the possibility to perform deep-level transient spectroscopy measurements at the Technische Universität Dresden.

Open Access funding enabled and organized by Projekt DEAL.

Conflict of Interest

The authors declare no conflict of interest.

Data Availability Statement

The data that support the findings of this study are available from the corresponding author upon reasonable request.

Keywords

defects, deep-level transient spectroscopy, hydrogen, iron, minority carrier transient spectroscopy, silicon

Received: March 1, 2022
Revised: April 27, 2022
Published online: May 26, 2022

[1] A. A. Istratov, H. Hieslmair, E. R. Weber, *Appl. Phys. A* **1999**, *69*, 13.
[2] M. Sanati, N. Gonzalez Szwacki, S. K. Estreicher, *Phys. Rev. B* **2007**, *76*, 125204.
[3] N. Gonzalez Szwacki, M. Sanati, S. K. Estreicher, *Phys. Rev. B* **2008**, *78*, 113202.
[4] P. Santos, J. Coutinho, S. Öberg, *J. Appl. Phys.* **2018**, *123*, 245703.
[5] A. J. Tavendale, S. J. Pearton, *J. Phys. C* **1983**, *16*, 1665.
[6] S. J. Pearton, A. J. Tavendale, *J. Phys. C* **1984**, *17*, 6701.
[7] M. Kouketsu, K. Watanabe, S. Isomae, *Mater. Sci. Forum* **1995**, *196–201*, 861.
[8] M. Kouketsu, S. Isomae, *J. Appl. Phys.* **1996**, *80*, 1485.
[9] O. V. Feklisova, A. L. Parakhonsky, E. B. Yakimov, J. Weber, *Mater. Sci. Eng. B* **2000**, *71*, 268.
[10] T. Sadoh, K. Tsukamoto, A. Baba, D. Bai, A. Kenjo, T. Tsurushima, H. Mori, H. Nakashima, *J. Appl. Phys.* **1997**, *82*, 3828.
[11] S. Leonard, V. P. Markevich, A. R. Peaker, B. Hamilton, J. D. Murphy, *Appl. Phys. Lett.* **2015**, *107*, 032103 .
[12] R. Stübner, V. Kolkovsky, J. Weber, *J. Appl. Phys.* **2015**, *118*, 055704.
[13] J. I. Pankove, D. E. Carlson, J. E. Berkeyheiser, R. O. Wance, *Phys. Rev. Lett.* **1983**, *51*, 2224.
[14] L. Scheffler, Vl. Kolkovsky, J. Weber, *J. Appl. Phys.* **2014**, *116*, 173704.
[15] L. Scheffler, Vl. Kolkovsky, J. Weber, *Phys. Stat. Sol. A* **2012**, *209*, 1913.
[16] L. Scheffler, Vl. Kolkovsky, J. Weber, *J. Appl. Phys.* **2013**, *113*, 183714.
[17] L. Scheffler, Vl. Kolkovsky, J. Weber, *J. Appl. Phys.* **2015**, *117*, 085707.
[18] K. Nakashima, M. Chijiiwa, *Jpn. J. Appl. Phys.* **1986**, *25*, 234.
[19] S. Tanaka, H. Kitagawa, *Jpn. J. Appl. Phys.* **1995**, *34*, L721.
[20] K. Kakishita, K. Kawakami, S. Suzuki, E. Ohta, M. Sakata, *J. Appl. Phys.* **1989**, *65*, 3923.
[21] V. V. Voronkov, R. Falster, *J. Cryst. Growth* **1998**, *194*, 76.
[22] G. Langouche, *Hyperfine Interact.* **1992**, *72*, 217.
[23] D. J. Silva, U. Wahl, J. G. Correia, J. P. Araujo, *J. Appl. Phys.* **2013**, *114*, 103503.
[24] S. H. Muller, G. M. Tuynman, E. G. Sieverts, C. A. J. Ammerlaan, *Phys. Rev. B* **1982**, *25*, 25.
[25] S. K. Estreicher, M. Sanati, N. Gonzalez Szwacki, *Phys. Rev. B* **2008**, *77*, 125214.
[26] O. Feklisova, N. Yarykin, *Semicond. Sci. Technol.* **1997**, *12*, 742.
[27] K. Gwozdz, V. Kolkovsky, V. Kolkovsky, J. Weber, *J. Appl. Phys.* **2018**, *124*, 015701.
[28] K. Gwozdz, V. Kolkovsky, *Phys. Status Solidi A* **2021**, *2100217*, 1.
[29] R. Stübner, V. Kolkovsky, J. Weber, N. V. Abrosimov, C. M. Stanley, D. J. Backlund, S. K. Estreicher, *J. Appl. Phys.* **2020**, *127*, 045701.
[30] V. P. Markevich, M. V. Contreras, J. Mullins, M. Halsall, B. Hamilton, L. I. Murin, R. Falster, J. Binns, E. Good, J. Coutinho, J. Medford, C. L. Reynolds, A. R. Peaker, in *2016 IEEE 43rd PV Spec. Conf.* IEEE, New York City at 3 Park Ave, United States **2016**, p. 688.
[31] L. Dobaczewski, A. R. Peaker, K. Bonde Nielsen, *J. Appl. Phys.* **2004**, *96*, 4689.
[32] P. Blood, P. W. Orton, *The Electrical Characterization of Semiconductors: Majority Carriers and Electron States*, Academic Press London, England **1992**.